International Journal of Astrobiology 5 (4): 333–342 (2006) Printed in the United Kingdom
doi:10.1017/S1473550406003466 First published online 14 November 2006

The ~3.4 billion-year-old Strelley Pool Sandstone: a new window into early life on Earth

David Wacey[1], Nicola McLoughlin[1], Owen R. Green[1], John Parnell[2], Crispin A. Stoakes[3] & Martin D. Brasier[1]

[1]*Department of Earth Sciences, University of Oxford, Parks Road, Oxford OX1 3PR, UK*
e-mail: davidwa@earth.ox.ac.uk
[2]*Department of Geology and Petroleum Geology, University of Aberdeen, Aberdeen AB24 3UE, UK*
[3]*C.A. Stoakes and Associates Pty Ltd, 3185 Victoria Road, Hovea, WA 6071, Australia*

Abstract: The recognition and understanding of the early fossil record on Earth is vital to the success of missions searching for life on other planets. Despite this, the evidence for life on Earth before ~3.0 Ga remains controversial. The discovery of new windows of preservation in the rock record more than 3.0 Ga would therefore be helpful to enhance our understanding of the context for the earliest life on Earth. Here we report one such discovery, a ~3.4 Ga sandstone at the base of the Strelley Pool Formation from the Pilbara of Western Australia, in which micrometre-sized tubular structures preserve putative evidence of biogenicity. Detailed geological mapping and petrography reveals the depositional and early diagenetic history of the host sandstone. We demonstrate that the depositional environment was conducive to life and that sandstone clasts containing putative biological structures can be protected from later metamorphic events, preserving earlier biological signals. We conclude from this that sandstones have an exciting taphonomic potential both on early Earth and beyond.

Received 28 June 2006, accepted 28 August 2006

Key words: Archaean, early life, microtubes, Pilbara, sandstone, Strelley Pool Formation, taphonomy.

Introduction

Identifying the first evidence for life on Earth is a task of considerable difficulty and one that must be approached with the utmost rigour (Buick 1990; Brasier *et al*. 2004). Critical to the assessment of the biogenicity and antiquity of any micrometre-sized structure is the geological and depositional setting of the host rock unit and its subsequent diagenetic history. For example, detailed mapping by Brasier *et al*. (2002, 2005) of the world famous 3.46 Ga Apex Chert 'microfossil site' found this site to occur some 100 m down a hydrothermal dyke system, not in a lagoonal or evaporitic setting as originally thought (Schopf & Packer 1987; Schopf 1993, 1999). Interpretation of these putative microfossils to include 'probable cyanobacteria' (Schopf 1999) was subsequently shown to be implausible for a wide range of reasons (Brasier *et al*. 2005). There has recently been renewed interest in the importance of hydrothermal and volcanic rocks as possible sites for carbonaceous fossil microbes (e.g. Walsh 2004) and this has been reinforced by the observations of biologically mediated microtubular structures in modern (Fisk *et al*. 1998) and ancient (Furnes *et al*. 2004, 2006) pillow lavas and hyaloclastites. In this paper, however, we use well-preserved sandstone from the Pilbara craton of Western Australia to demonstrate that *sediments* remain one of the best candidate lithologies in which to search for evidence of early life.

The Pilbara craton contains some of the Earth's best-preserved stratigraphic successions of early Archaean rocks, including sediments more than 3.5 Ga (Bjonnes & Lindsay 2005) and some of the oldest indisputable sandstones (Lowe 1983). The craton was an Archaean proto-continent (Smithies *et al*. 2005), resulting from mantle plume events, consisting of granitoid bodies emplaced into and overlain by the Pilbara Supergroup (Van Kranendonk *et al*. 2001). The oldest part of the craton is the East Pilbara granite–greenstone terrain (Fig. 1(a)) comprising ~3.655–2.85 Ga granitoid bodies, and an almost contemporaneous ~3.515–3.0 Ga volcanogenic carapace and associated sediments (Pilbara Supergroup) now preserved as several greenstone belts (Van Kranendonk 2006). In detail, the Pilbara Supergroup contains four unconformity bound stratigraphic intervals (groups): the ~3.515–3.427 Ga Warrawoona Group, the ~3.40–3.315 Ga Kelly Group, the ~3.24 Ga Sulphur Springs Group and the ~3.2–3.0 Ga Gorge Creek Group (see fig. 2 of Van Kranendonk (2006)). Each of the four groups were deposited on top of one another and consistently dip away from the domal granitoids. The dips

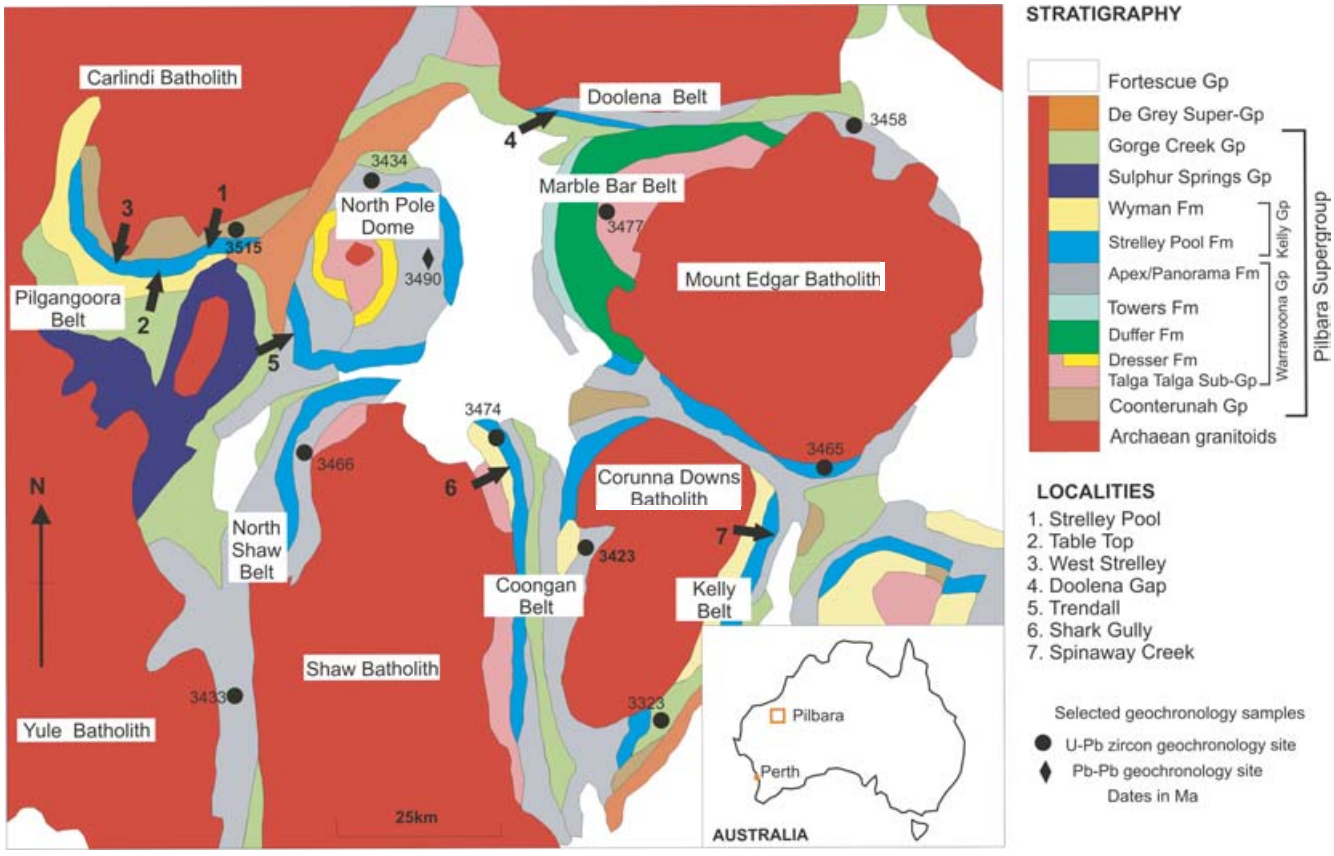

(a)

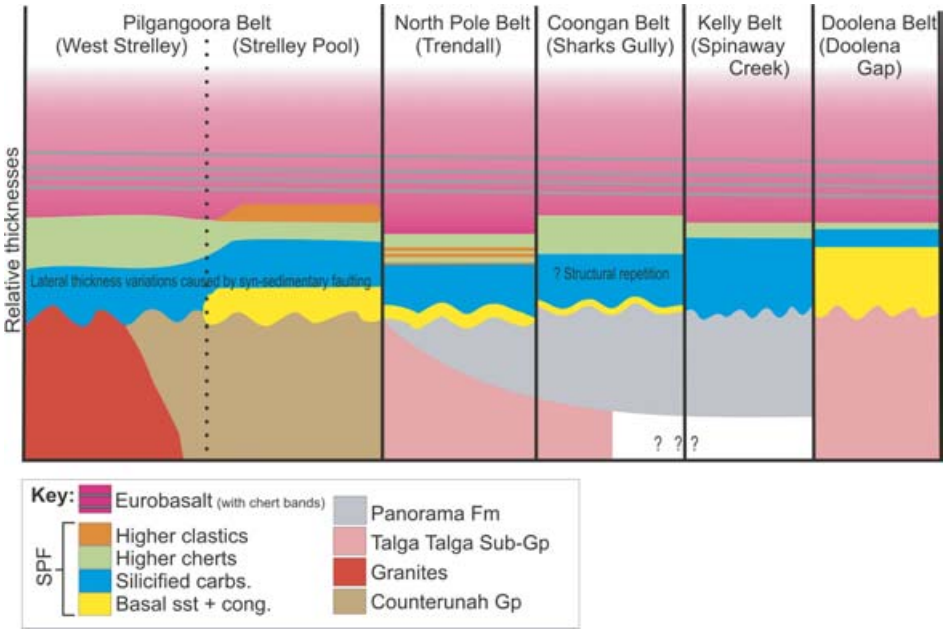

(b)

Fig. 1. Regional setting of the SPF. (a) Geological sketch map of the East Pilbara granite–greenstone terrain (modified from Van Kranendonk *et al.* (2001)). (b) Comparative cross-sections through five of the greenstone belts showing the distribution of the Strelley Pool Sandstone Member (SPFS) and adjacent stratigraphic units.

https://doi.org/10.1017/S1473550406003466 Published online by Cambridge University Press

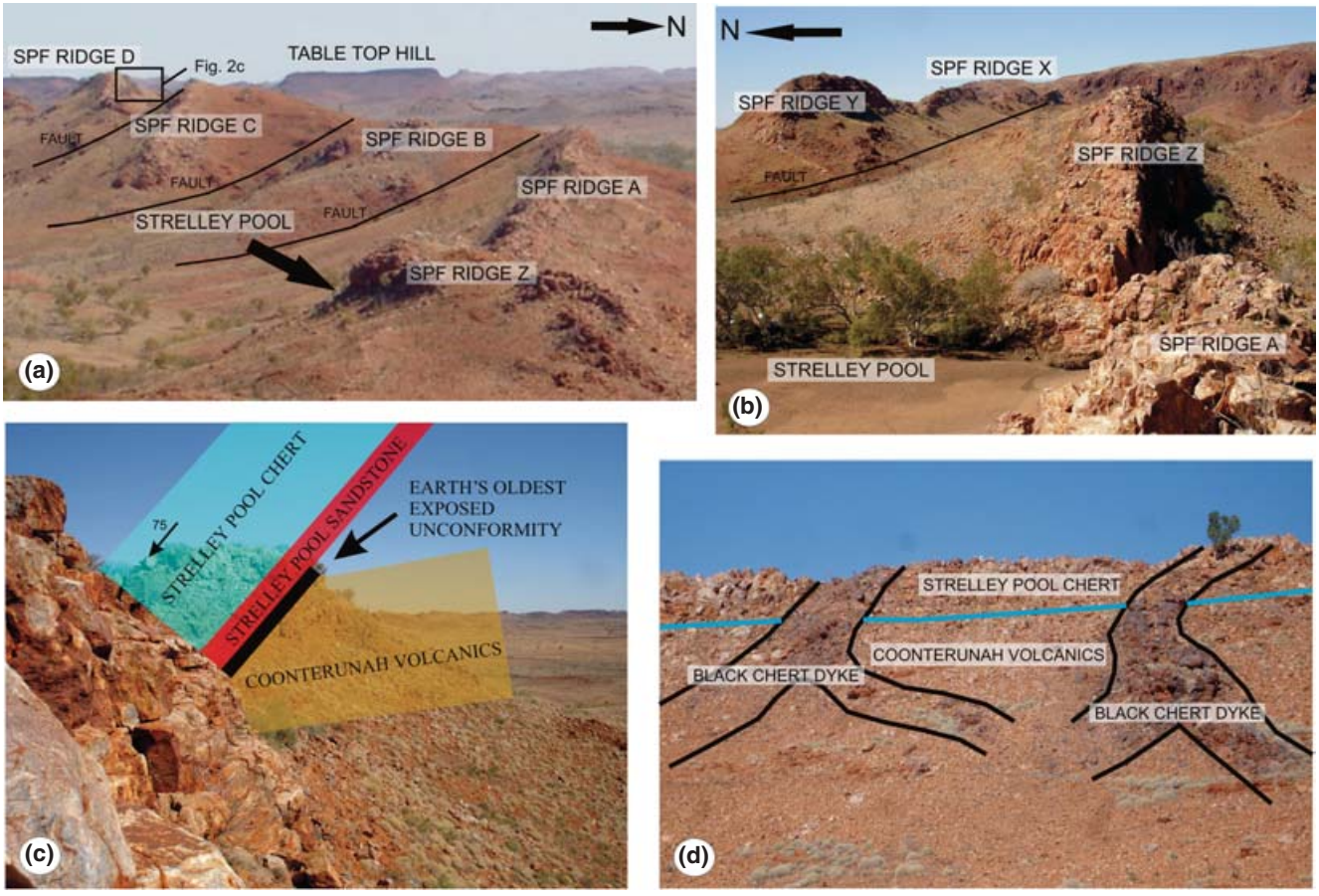

Fig. 2. Field relations of the SPF. (a) Photograph looking west showing the location of Strelley Pool and of the ridges to the west of Strelley Pool referred to in Figs 4–6 and in the text. (b) Photograph looking east showing the location of the ridges to the east of Strelley Pool referred to in Figs 4–6 and in the text. (c) Photograph looking west across ridge D showing Earth's oldest exposed unconformity between 3.515 Ga Coonterunah Group volcanics and the ~3.4 Ga SPFS. (d) Photograph looking south at a ridge of SPF (that has no basal sandstone) unconformably overlying the Coonterunah volcanics. Here, black chert dykes cross cut both the volcanics and the laminated chert, but do not penetrate the overlying Eurobasalt Formation.

gradually decrease with time suggesting deposition as thickening wedges adjacent to the growing granitoid diapirs (Hickman 1975, 1983, 1984; Van Kranendonk 1999, 2000; Van Kranendonk *et al*. 2002).

We have discovered micrometre-sized tubular structures within a sandstone at the base of the Strelley Pool Chert Formation within the Kelly Group. Here we wish to redefine the Formation in which these structures occur. The use of 'Chert' in the Formation status is misleading as our mapping shows the Formation (Fig. 3) to comprise: (1) basal silicified sandstone and conglomerate; (2) silicified carbonate; (3) laminated chert; and (4) upper clastics. We therefore advocate the removal of the word 'Chert' from the Formation status. Thus, the Strelley Pool Chert Formation simplifies to the Strelley Pool Formation (SPF). The microtubes occur in the basal sandstone unit, here named the Strelley Pool Sandstone Member (SPFS) of the SPF. Below we present a description of the geological distribution, structure and petrography of the SPFS, and an outline for the environment of deposition and early diagenetic history.

Distribution and structure of the Strelley Pool Sandstone Member

Field mapping

Our field mapping shows that the SPFS occurs as a discontinuous member at the base of the ~3.4 Ga SPF within the Kelly Group, which outcrops throughout several parts of the East Pilbara granite–greenstone terrain (Fig. 1(b)). It varies in thickness from less than 1 m in parts of the Coongan and North Shaw Belts to over 500 m in the Doolena Belt. This contrasts substantially with the overlying silicified laminated carbonate and chert members of the SPF, which can be mapped at a relatively constant thickness of ~25 m across the terrain (Van Kranendonk 2006).

At the type locality of Strelley Pool in the Pilgangoora Belt (Locality 1, Fig. 1(a)) the SPFS is up to 5 m thick and was deposited unconformably over 3.515 Ga volcanics of the Coonterunah Group (Figs 1(b) and 2(c)). This unconformity surface records the earliest period of subaerial exposure and chemical weathering in the rock record (Buick *et al*. 1995) and

https://doi.org/10.1017/S1473550406003466 Published online by Cambridge University Press

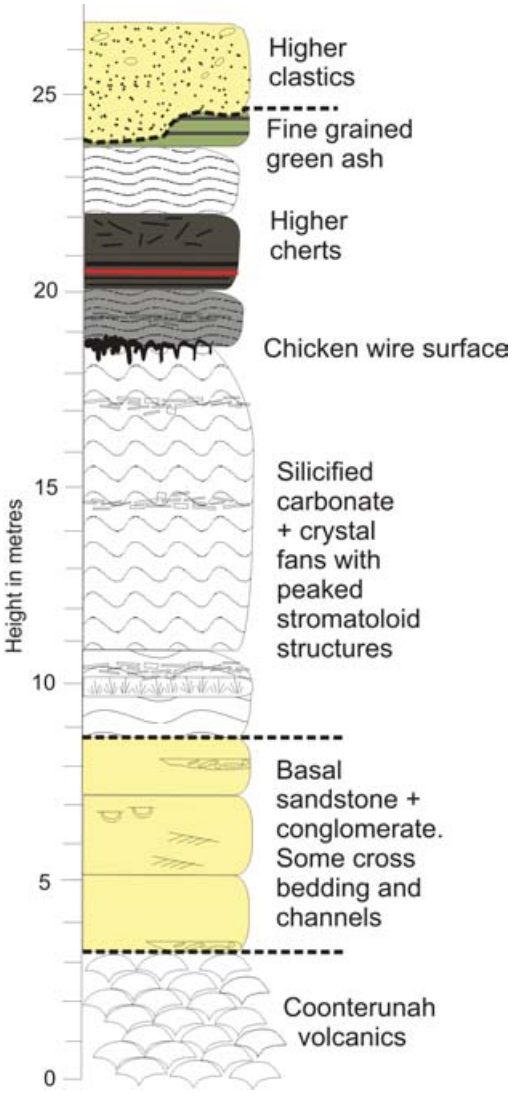

Fig. 3. Stratigraphic log of the SPF at the type locality of Strelley Pool. Note that this is a mixed carbonate/clastic deposit and that the thicknesses of the basal sandstone and conglomerate vary along strike.

the sandstone appears to infill channels and hollows in the ancient topography. Occasionally, relic topography is still seen at the top of the SPFS and here the overlying chert member forms drape structures (Fig. 4(a)) over the SPFS.

Around Strelley Pool, a basal conglomerate is locally present within the SPFS; containing large sub-rounded clasts of the basement rock (Fig. 5(a)), plus clasts of jaspilitic chert (Fig. 5(b)). Above this, the sandstone shows both fining-upwards sequences and coarsening-upwards sequences (see Fig. 6) in close proximity to one another along strike. Two distinct sandstone lithologies can be distinguished by colour in outcrop, with lenses of grey to black sandstone occurring as localized pods within the more common grey–green sandstone (Fig. 5(d)). Petrographic study is required to distinguish them further (refer to the 'Sandstone petrography' section). Cross bedding is still visible in numerous places in both the black and grey–green sandstones (Fig. 4(c)) but can often be obscured by the silicification process.

Along the strike from Strelley Pool, within the Pilgangoora Belt, the sandstone pinches and swells, presumably in relation to the ancient topography of the basement and the distribution of numerous local syn-depositional growth faults (Figs 2(a) and (b)). East of Strelley Pool the sandstone is present more or less continuously for 8 km until the SPF is faulted out against the Lalla Rookh Sandstone of the De Grey Group. To the west, however, broad regional thinning is observed where the SPFS occurs as a thin quartz arenite (Fig. 6(c)) around Table Top Hill (Locality 2, Fig. 1(a)). Yet further west, at the West Strelley River (Locality 3, Fig. 1(a)), some 15 km to the west of Strelley Pool, the SPFS thins to nothing. Where the SPFS is absent, laminated silicified carbonates lie unconformably on the Coonterunah Group or the Carlindie Granite (Fig. 1(b)). Numerous black chert dykes intrude and interfinger with these laminated chert ridges (Fig. 2(d)).

The SPFS is thickest at Doolena Gap within the Doolena Belt (Locality 4, Fig. 1(a)). Here the unit is up to 500 m thick, bedded on a metre scale and exhibiting large-scale channel structures (Fig. 4(d)). Low-angle cross bedding is weakly developed here. The sandstone is more heavily silicified than at Strelley Pool, exhibiting a rather uniform medium- to coarse-grained sugary texture. At the Trendall Locality in the North Shaw Belt (Locality 5, Fig. 1(a)), and at Sharks Gully in the Coongan Belt (Locality 6, Fig. 1(a)), the SPFS is only present locally. At both localities it is less than 2 m thick, and has yet to be studied in detail. Further south, around Spinaway Creek in the Kelly Belt (Locality 7, Fig. 1(a)), the SPFS is completely absent.

The microtubes

Our discovery of microtubes from the ~3.4 Ga SPFS has opened up a new taphonomic window within which to critically examine the evidence for early life. The microtubes themselves have been described in Brasier *et al.* (2006), whilst the geochemical and petrographic evidence used to investigate their putative biogenicity is largely presented elsewhere (Wacey *et al.* submitted). However, to illustrate the importance of these structures, a brief summary of their distribution, morphology and chemical composition is included here. We then present a petrographic study of the sandstones and conglomerates of the SPFS, focusing on the compositional and textural maturity of the sediments and what this can tell us about the preservational pathways, i.e. the taphonomy of putative microtubular biosignatures preserved in sandstones.

The microtubes are restricted to a distinct type of early formed, well-rounded clasts of microcrystalline silica whose texture indicates a volcanic source (Fig. 5(f)). The morphology of the microtubes varies between two end members, Type A and Type B. Type A are linear and narrow (1–10 μm width, 5 μm modal width and up to 200 μm long) with pointed to blunt terminations; they sometimes occur in clusters directed away from clots of organic-rich material (Fig. 5(g)).

https://doi.org/10.1017/S1473550406003466 Published online by Cambridge University Press

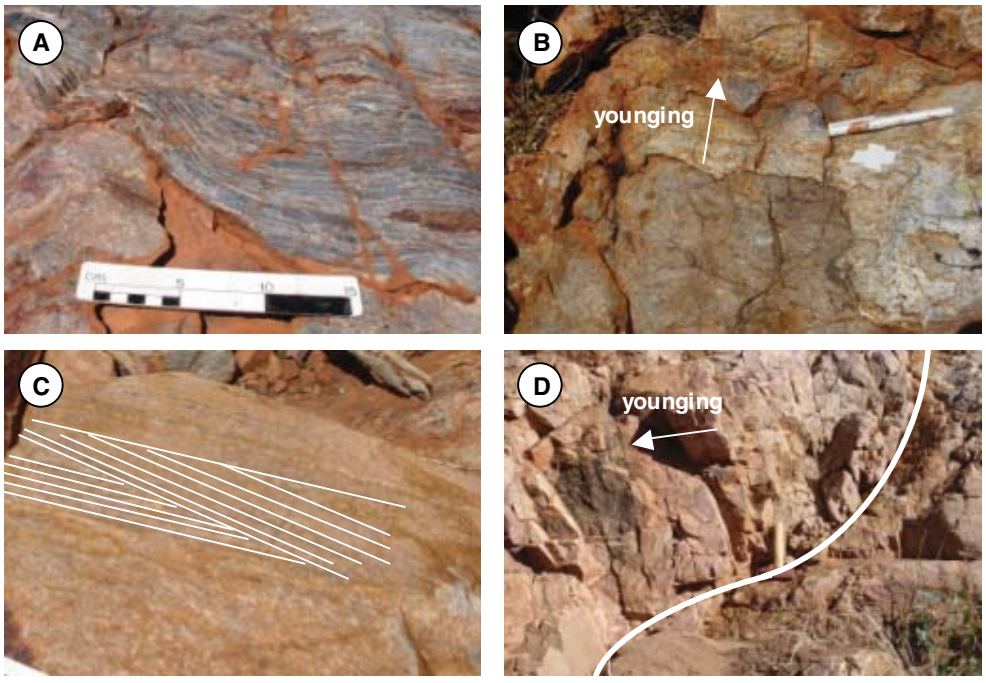

Fig. 4. Structures within the SPF. (a) Layered chert draping over a channel within the basal sandstone on ridge Y. (b) Soft sediment deformation indicated by the loading structure of chert into sandstone on ridge D (the pen is 15 cm long). (c) Low-angle laminar cross bedding (mm to cm scale) within the SPFS on ridge D (the scale is the same as for (a)). (d) Channel within the SPFS at Doolena Gap (the hammer is 50 cm long).

Type B microtubes are much more varied in morphology. They may be straight, curved, twisted or helical and can occur on their own or in tangled clusters (Fig. 5(g)). They also tend to be slightly larger (2–15 μm width, 9 μm modal width and up to 100 μm long) and are more abundant than Type A microtubes. Both types of microtube exhibit carbon- and nitrogen-rich linings (Wacey *et al*. 2006) and can be partially or totally infilled with either iron- or aluminium-phosphate, or iron-rich sulphate. Their morphology, distribution and geochemistry are suggestive of a biogenic component to their formation (Brasier *et al*. 2006; Wacey *et al*. 2006) but further investigation is necessary to confirm this. Some of the Type B tubes contain pyrite grains associated with carbon at their terminations, consistent with a biologically mediated ambient inclusion trail mechanism for their formation (cf. Knoll & Barghoorn 1974). The remainder may be mediated by etching and boring by primitive endolithic bacteria akin to similar structures described both in modern (Fisk *et al*. 1998) and early Archaean (Furnes *et al*. 2004, 2006) pillow lavas.

Microtube localities

Microtubes have so far only been discovered within the SPFS in the vicinity of Strelley Pool (Locality 1, Fig. 1(a)). Here, the SPF is easily recognized; it dips at ~75–85° S, and forms a narrow ridge trending east–west and is offset by numerous faults that cut the stratigraphy at a high angle (Figs 2(a) and (b)). For ease of description, we have assigned alphabetical letters to each of the fault-bounded blocks (A to E, due west of Strelley Pool, Fig. 2(a); and Z to X, due east of Strelley Pool, Fig. 2(b)).

The silicified carbonate and chert members of the SPF (Fig. 3) have received particular attention in the literature because they contain coniform stromatoloid structures that have been argued, mainly on morphological grounds, to be evidence for early life (Lowe 1980; Hofmann *et al*. 1999; Hofmann 2000; Allwood *et al*. 2006). These structures are controversial and abiogenic mechanisms for their formation have also been postulated (Lowe 1994; Brasier *et al*. 2006). Surprisingly, there are no previous reports of biogenic structures in the SPFS, although there have been short geological descriptions in Lowe (1983) and Van Kranendonk (2000).

Sandstone petrography

A full understanding of the context of putative biogenic structures within any ancient rock type can only be achieved with a comprehensive petrographic thin-section analysis. Figure 6 shows a ternary diagram based on point counts of 12 different SPFS samples from the vicinity of Strelley Pool and associated photomicrographs.

It can be seen that the majority of samples plot towards the quartz-rich part of the triangle, many in the fields of sublitharenite and litharenite with a minority that are subarkosic. The figure also shows that the samples containing microtubes occur in a natural group clustered along the quartz-rock fragment axis and do not occur in the more quartz- or

https://doi.org/10.1017/S1473550406003466 Published online by Cambridge University Press

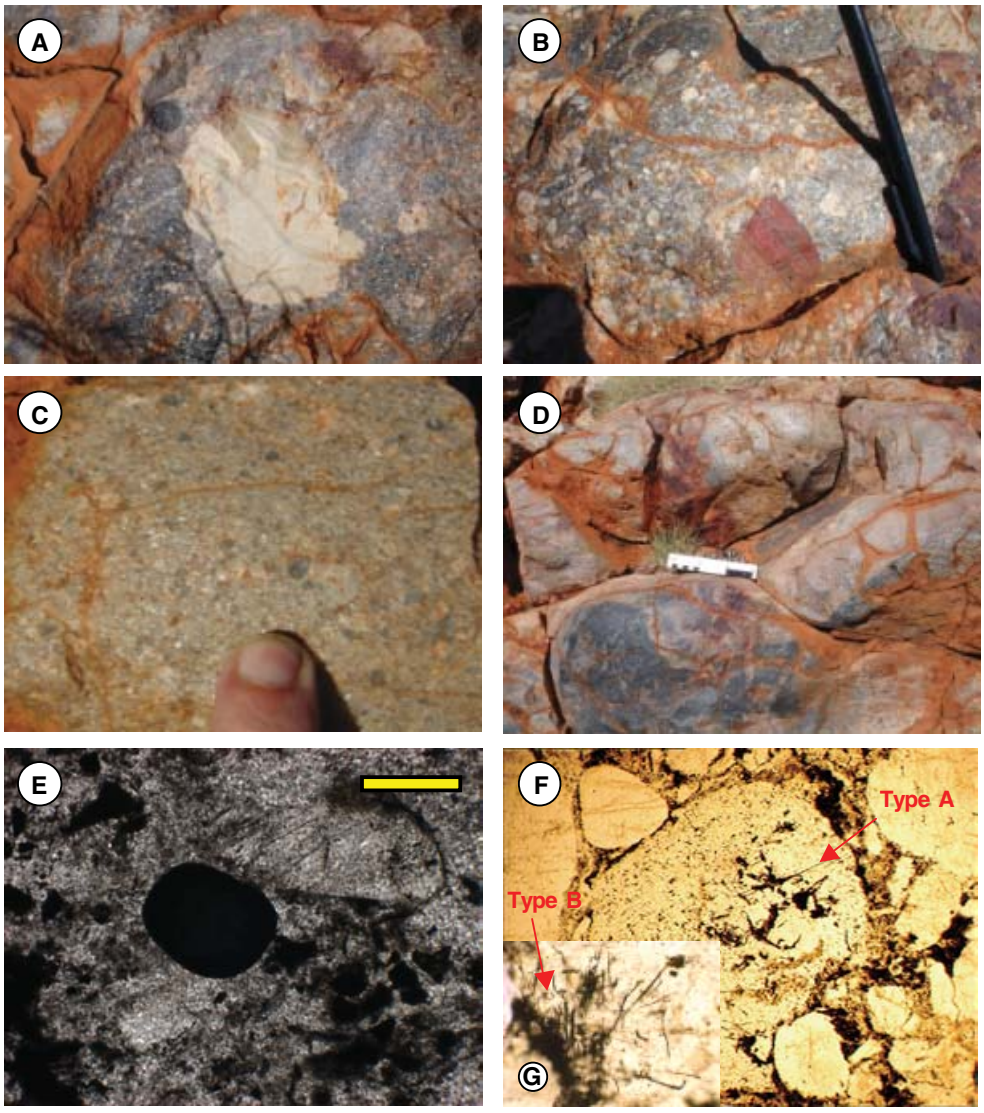

Fig. 5. Photographs of SPFS lithology. (a) Basal conglomerate from ridge A with a large (5 cm), rather angular rip-up clast from the underlying Coonterunah Group. (b) Basal conglomerate from ridge A with 3 cm clast of jaspilitic chert. (c) Close-up of coarse-grained SPFS from ridge D – note the well-rounded dark-grey grains, some of which contain microtubes (the finger is 2 cm across). (d) Lense of black sandstone within more common grey–green sandstone from ridge Y (the scale marker is 15 cm). (e) Photomicrograph of the black sandstone – in thin section the black colouration is seen to be the result of high concentrations of pyrite and carbon (the scale bar represents 200 μm). (f) Photomicrograph of a well-rounded grain containing microtubes from ridge D (the scale bar represents 300 μm). (g) Inset, morphology of the microtubes showing both Type A and Type B microtubes clustering and emanating from a clot of organic-rich material (lower left); the scale bar represents 200 μm.

feldspar-rich lithologies. This indicates that the mineralogical components of the sandstone are of importance, with the vast majority of the microtubes occurring in dark-grey, metal-rich, microcrystalline silica grains of inferred volcanic origin. Likewise, the grain size and sorting of the sandstone is seen to be important with the majority of the microtubes restricted to coarse-grained, but moderately sorted, sandstone in which some matrix component is still present. All other microtube-containing samples have closely comparable petrographic characteristics. Details of the non-microtube-containing lithologies are contained within Fig. 6, whilst the microtube-containing lithology is described below.

The lithology containing the microtubes (Figs 5(c) and 6(e)–(h)) is a coarse-grained, moderately sorted, quartz-rich sandstone with conspicuous lithic grains of dark-grey microcrystalline silica (e.g. top left and bottom right of Fig. 6(e)) up to 4 mm in size. The framework grains are well rounded and set in a matrix of finer quartz, probable altered feldspar and volcanics, and phosphate. SP9 (Fig. 6(e)) is the original sample that was found to contain microtubes, collected in 2003 from ridge D (Figs 2(a) and (c)) by NM. The microtubes were observed to only occur in the dark-grey microcrystalline silica grains. In 2005 DW, ORG and MDB, with the aid of a photograph taken by NM, relocated the SP9 site and collected more material from along strike and up section. SP9i

https://doi.org/10.1017/S1473550406003466 Published online by Cambridge University Press

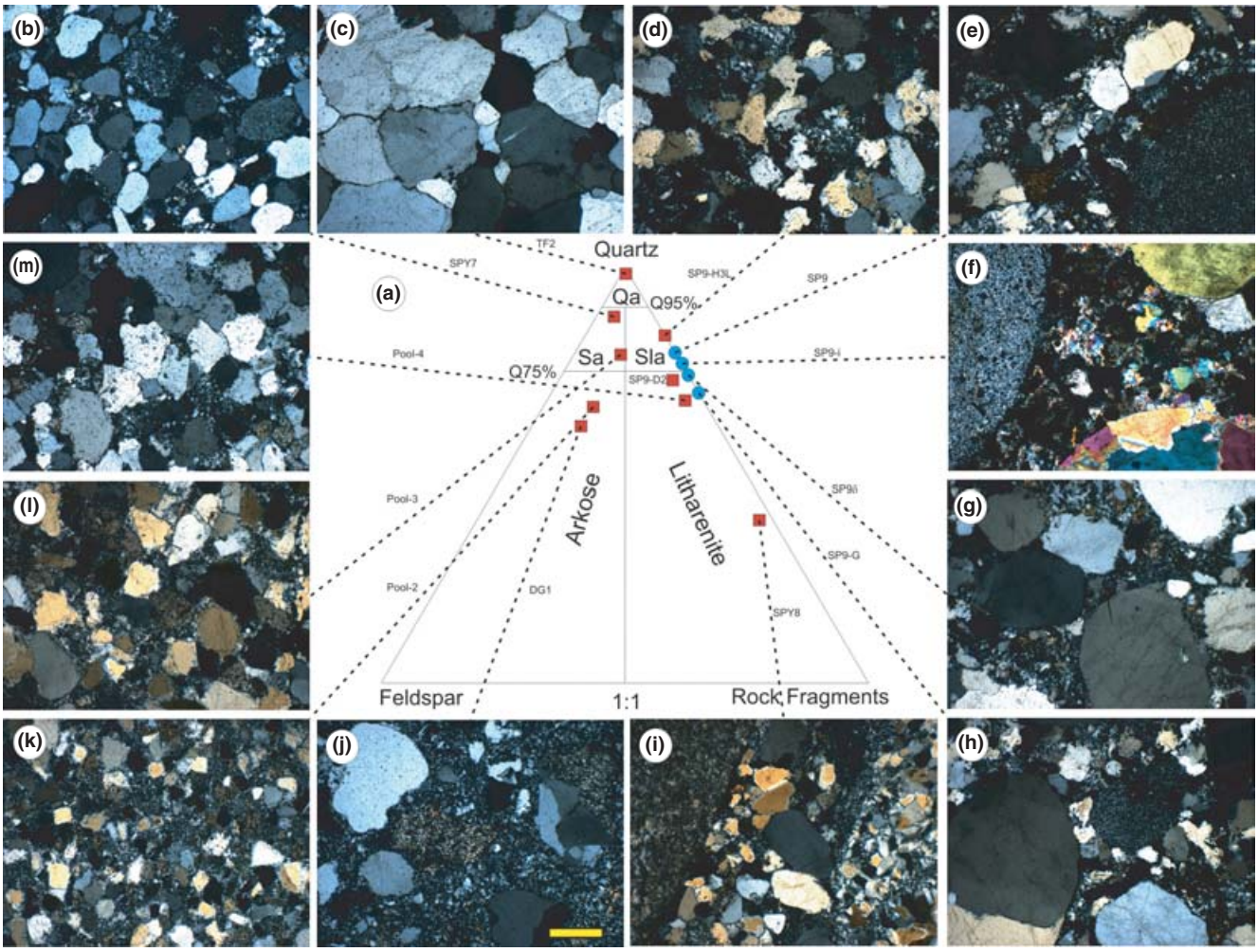

Fig. 6. Petrography of the SPFS. All images were taken under cross-polarized light at ×4 magnification using a Nikon Optiophot-pol (polarizing) microscope, imaged with a QI digital 12 bit colour camera and processed using AcQuis image-capturing software. Mineralogical composition was estimated using the Gazzi–Dickinson method of point counting (Gazzi 1966; Dickinson 1970; Ingersoll et al. 1984), using 300 point counts per thin section. (a) Ternary sandstone classification diagram based on relative percentage of constituent framework minerals (after Folk 1968): Qa = quartz arenite, Sa = sub-arkose, Sla = sub-litharenite, circles = microtube containing samples, squares = samples without microtubes. (b) Grey–black sub-arkose from ridge Y, which shows centimetre-scale, low-angle laminar cross bedding in a hand specimen. It is a well-sorted, mature, quartz-rich sandstone with occasional altered feldspar and lithic volcanic grains (sample SPY7). (c) Grey quartz arenite from Table Top Hill (sample TF2), collected from directly below a Tertiary ferricrete deposit. It is very well indurated and composed of almost 100% quartz grains, up to 1 mm in diameter, with a small amount of matrix, now sandwiched between sutured quartz boundaries. On the surface it is heavily iron stained and this staining persists as an oxidation front into the first 2 cm of the rock. (d) Moderately sorted sub-litharenite from ridge D near Strelley Pool showing some suturing of quartz grain boundaries (sample SP9-H3L). (e) Moderately sorted sub-litharenite with large well-rounded lithic-volcanic grains (containing microtubes) from ridge D near Strelley Pool (sample SP9). (f) Moderately sorted sub-litharenite with phosphate-rich matrix and large well-rounded lithic-volcanic grains (containing microtubes) from ridge D near Strelley Pool (sample SP9i). (g) Moderately sorted litharenite showing large well-rounded monocrystalline quartz grains from ridge D near Strelley Pool (sample SP9δ). (h) Litharenite with a well-rounded volcanic grain (centre) from ridge D near Strelley Pool (sample SP9G). (i) Dark-grey conglomerate from ridge Y (sample SPY8) containing clasts of silicified volcanic ash, volcanic glass, jaspilitic chert and megaquartz. The clasts are well rounded, the majority being in the 5–15 mm size range. It is grain supported by sand-sized monocrystalline quartz grains which are also moderately well rounded. (j) Grey–pink lithic arkose sandstone from Doolena Gap (sample DG1) which is heavily silicified giving a sugary texture and some conchoidal fracturing. It is composed of sub-rounded mono- and poly-crystalline quartz grains up to 1 mm in diameter that are moderately well sorted, plus heavily altered feldspar and rare volcanic fragments. It has a microcrystalline quartz cement, some fine quartz veining and a little iron staining. (k) Fine-grained, well-cemented, well-sorted grey arkosic sandstone (sample Pool-2) from ridge Z, dominated by sub-angular to sub-rounded quartz grains less than 0.2 mm in size. Occasional altered feldspar and volcanic fragments are also present set in a microcrystalline quartz cement. (l) Grey–green sub-arkosic sandstone (sample Pool-3) from 50 cm above Pool-2 on ridge Z. It is dominated by well-sorted quartz grains that are larger (up to 0.6 mm) and more rounded than in Pool-2. Altered feldspar and volcanic fragments contribute around 20% of the framework grains. It is well cemented by microcrystalline quartz, and was the hardest of all samples to hammer in the field. (m) Grey–green litharenite (sample Pool-4) from 2 m stratigraphically above Pool-3 at the top of the SPCs. It is dominated by monocrystalline quartz which is slightly coarser (averaging 1 mm) than Pool-3 (continuing the coarsening upwards sequence of this ridge). There is very little feldspar, only occasional volcanic fragments and little matrix or cement; the quartz grains often have sutured contacts with one another. Occasionally it contains pods (greater than 1 cm) of black sandstone enriched in carbon and pyrite. The scale bar is 0.5 mm long.

https://doi.org/10.1017/S1473550406003466 Published online by Cambridge University Press

(Fig. 6(f)) comes from immediately adjacent to SP9 and exhibits all the same textural and mineralogical features as SP9. Microtubes again occur in the dark-grey grains and rarely also in megaquartz grains. SP9G (Fig. 6(h)) was collected from the same stratigraphic height as SP9, but 10 m to the west along ridge D. Once again it is a coarse-grained lithic sandstone, slightly finer grained than SP9 and slightly richer in lithic grains. In all other ways it is identical to SP9 and again contains microtubes that are confined to the lithic microcrystalline silica grains. SP9-H3L (Fig. 6(d)) was collected from a locality 1 m directly above SP9 and is texturally very different. It is much finer grained, darker in colour and lacks the conspicuous well-rounded lithic grains of SP9; instead it closely resembles SPY7 (Fig. 6(b)) from ridge Y, and lacks microtubes. A black sandstone from ridge D (Sample SP9-D2, Fig. 6(a)) is notable for its concentration of pyrite. The framework mineralogy, dominated by quartz with some lithic fragments, and texture are very similar to other SP9 samples (Fig. 6(a)) but it contains no microtubes. Instead it contains micrometre-sized pyrite crystals, associated with carbon, that coat many of the quartz framework grains. Occasional larger pyrite grains occur in several samples. They range from rather angular, to sub-rounded, to very well-rounded grains and appear detrital in origin (Fig. 5(e)).

Coupled petrographic and fluid inclusion studies show that, post deposition, the sandstone experienced a normal history for a siliciclastic rock with cementation (overgrowth), pressure solution, micro-fracturing and fracture-healing over a temperature range of up to 150 °C. This record has not been disturbed or overprinted by metamorphism, with the sandstone only experiencing tilting and heating to prehnite–pumpyllite facies as the granitoid domes continued to rise.

Environment of deposition of the SPFS

The mapping and sedimentological data presented above can be used to help formulate a depositional model for the SPFS. We note the following macroscopic features within the SPFS consistent with shallow water, high-energy deposition: (1) cross bedding, arranged in truncated sets, consistent with strong bottom currents; (2) relatively shallow scour-and-fill channel structures possibly produced by rip currents; (3) textural maturity shown by moderately to well-sorted, sub-rounded to well-rounded grains, consistent with effective sorting and winnowing; (4) compositional maturity shown by the quartz-dominated grains, resulting from prolonged mechanical and chemical breakdown; and (5) spatially restricted conglomeratic lag deposit containing large clasts of the basement rock, again consistent with a high-energy environment.

Two possible models can be put forward to explain these observations: the first is a beach-like setting (Lowe 1983); the second is a sub-tidal coastal sand blanket formed in response to storms and waves. Although our current evidence is in agreement with Lowe (1983), further observations are needed before we can confidently reject the second (mainly sub-tidal)

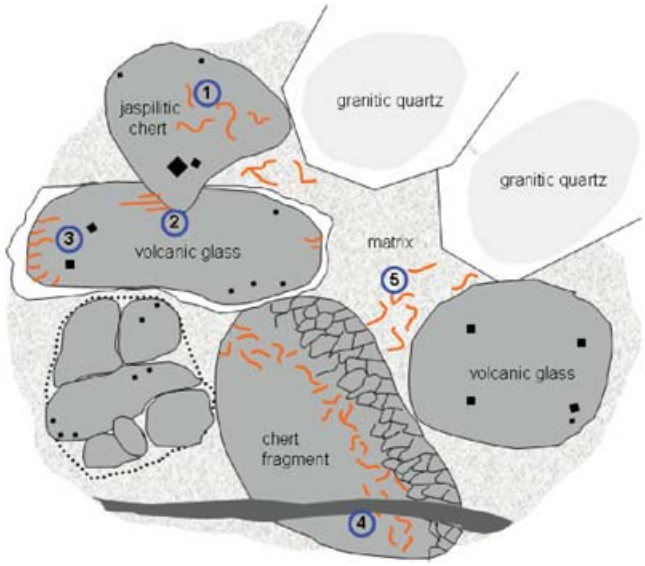

Fig. 7. Schematic diagram demonstrating the age relationships between putative biogenic structures and major textural components of a sandstone or conglomerate: (1) structures pre-date deposition; (2) structures pre-date or are penecontemporaneous with compaction; (3) structures pre-date mineral overgrowths; (4) structures pre-date the vein; (5) structures may be syn-depositional – further supporting evidence needed.

model. Either way, the basal sandstones and conglomerates were clearly deposited as a shallow marine transgression across a terrestrial unconformity surface. Variations in the grain size, sorting and thickness of these clastic units across the Pilbara greenstone terrain (refer to 'Field mapping' and 'Sandstone petrography' sections) are attributed here to differences in the local bathymetry and the rates of sediment supply.

Mapping identified rapid changes in grain size along strike and this is of particular interest. For example, on ridge D, the SPFS grain size becomes finer upwards, before the final cessation of clastic input. Conversely, grain size coarsens upwards on ridge Z. This implies that it is not merely a transgression in which deeper water and lower-energy environments become more dominant with time. The localized coarsening upwards, as observed on ridge Z, may indicate migration and progradation of coarse sand bars, possibly in response to fault control during deposition (cf. Nijman *et al.* 1998). In this respect it is interesting to note that the SPFS can thicken towards some faults, across which the unit either becomes very thin or disappears. We infer that there was a small component of syn-depositional faulting to explain these features in addition to later faulting that offsets the ridges.

The depositional context for the overlying chert members of the SPF appears to be similar to that inferred for the broadly coeval 3.416 Ga Buck Reef Chert of South Africa (Tice & Lowe 2004). Clastic sedimentation ceased, most likely in response to a major transgression. The water depths of deposition for the higher members of the SPF are not

https://doi.org/10.1017/S1473550406003466 Published online by Cambridge University Press

precisely constrained but were at or above the storm wave base, as indicated by abundant ripploid horizons, 'swaley' laminae and putatively storm-induced soft sediment deformation (Fig. 4(b)). Previous interpretations of an evaporitic setting (e.g. Lowe 1983) are not supported here; there is scarce evidence as yet for either desiccation cracks or exposure surfaces (contra Allwood *et al*. 2006).

The significance of sandstones as taphonomic windows for early life – establishing syngenicity

One of the most difficult tasks when studying putative biogenic structures in ancient rocks is establishing the syngenicity of the structure with the early depositional history of the rock. For example, in cherts, the most widely studied Archaean rock type, it is very difficult to untangle multiple generations of silica precipitation, dissolution and replacement, and there are seldom large-scale cross-cutting structures to aid interpretation. This can easily result in the misinterpretation of the depositional and diagenetic history of the rock and can have consequences for inferences of biogenicity. For example, putative microfossils from the 3.46 Ga Apex Chert were reported to occur in first generation fabrics (Schopf 1992, 1993, 1999) or in clasts deposited prior to its lithification (Schopf & Packer 1987). However, detailed petrographic mapping by Brasier *et al*. (2002, 2005) demonstrated that the majority of the putative microfossils occurred in second- and third-generation fabrics, thus casting doubt on their indigenous nature and inferred biogenicity.

However, clastic sedimentary rocks are more straightforward to interpret. Sandstones have clearly defined stages in their depositional and diagenetic history and structures found within sandstones can be matched with one or more of these stages using the conglomerate test. In this schematic example, shown for the Strelley Pool Sandstone (Fig. 7), the interpretation would be as follows: (1) structures found entirely within well-rounded framework clasts or grains must pre-date deposition of the sandstone (indeed they could be considerably older than the sandstone, dependent upon the age of the source rock); (2) structures truncated by grains impacting one another must either pre-date the compaction of the sediment or be synchronous with and driven by this compaction; (3) structures truncated by mineral overgrowths must have occurred prior to these overgrowths and thus pre-date compaction and pressure solution; (4) structures that are truncated by veins or fractures must pre-date the veins/fractures (the veins and fractures can themselves be constrained by observations of the types of grain in which they occur and whether they penetrate just one or multiple grains); (5) structures within the matrix are more difficult to constrain and must be interpreted with caution, especially if there are obvious later conduits for their entry into the rock. Not all of these relationships will be found in a single thin section, but careful observations over multiple thin sections will be able to constrain the age relationships of any structures present much better than in cherts or volcanic rocks of similar ages.

Conclusion

We have presented a geological and petrographic investigation of the 3.4 Ga Strelley Pool Sandstone and propose a new window into early life on Earth. Compared with the more common Archaean rock types of chert and pillow basalt, sandstones provide an additional and hitherto underappreciated taphonomic perspective on the early Earth. We therefore contend that ancient sandstones make particularly good future targets for the enhancement of our understanding of early biosphere processes on Earth and beyond.

Acknowledgements

We are grateful to the Geological Survey of Western Australia for extensive logistical support of our field program and to Arthur Hickman (GSWA), Martin Van Kranendonk (GSWA) and Kath Grey (GSWA) for generous advice and assistance. This study has benefited greatly from constructive discussions with Andrew Steele (Carnegie Institute, Washington), Stephen Moorbath (Oxford University) and John Lindsay (Lunar Planetary Institute, Houston). Fieldwork funding was variously received for MDB, NMcL, DW, and ORG from the Royal Society, NERC and the Oxford Burdett Couttes fund. DW is supported by a NERC grant and NMcL undertook this work as part of a NERC studentship.

References

Allwood, A.C., Walter, M.R., Kamber, B.S., Marshall, C.P. & Burch, I.W. (2006). Stromatolite reef from the early Archaean era of Australia. *Nature* **441**, 714–718.

Bjonnes, E. & Lindsay, J.F. (2005). The depositional setting of Earth's earliest sedimentary rocks. *Lunar Planet. Sci.* **XXXVI**, (Abstract) 1821.pdf.

Brasier, M.D., Green, O.R., Jephcoat, A.P., Kleppe, A.K., Van Kranendonk, M.J., Lindsay, J.F., Steele, A. & Grassineau, N.V. (2002). Questioning the evidence for Earth's oldest fossils. *Nature* **416**, 76–81.

Brasier, M.D., Green, O.R., Lindsay, J.F., McLoughlin, N., Steele, A. & Stoakes, C. (2005). Critical testing of Earth's oldest putative fossil assemblage from the ~3.5 Ga Apex Chert, Chinaman Creek Western Australia. *Precamb. Res.* **140**, 55–102.

Brasier, M.D., Green, O.R. & McLoughlin, N. (2004). Characterization and critical testing of potential microfossils from the early Earth: the Apex 'microfossil debate' and its lessons for Mars sample return. *Int. J. Astrobiol.* **3**, 139–150.

Brasier, M.D., McLoughlin, N., Green, O.R. & Wacey, D. (2006). A fresh look at the fossil evidence for early Archaean cellular life. *Phil. Trans. R. Soc. B*, **361**, 887–902.

Buick, R. (1990). Microfossil recognition in Archaean rocks: an appraisal of spheroids and filaments from 3500 M.Y old chert–barite at North Pole, Western Australia. *Palaios* **5**, 441–459.

Buick, R., Thornett, J.R., McNaughton, N.J., Smith, J.B., Barley, M.E. & Savage, M. (1995). Record of emergent continental crust ~3.5 billion years ago in the Pilbara craton of Australia, *Nature* **375**, 574–577.

Dickinson, W.R. (1970). Interpreting detrital modes of greywacke and arkose. *J Sed. Petrol.* **40**, 695–707.

Fisk, M.R., Giovannoni, S.J. & Thorseth, I.H. (1998). Alteration of oceanic volcanic glass: textural evidence of microbial activity. *Science* **281**, 978–980.

https://doi.org/10.1017/S1473550406003466 Published online by Cambridge University Press

Folk, R.L. (1968). *Petrology of Sedimentary Rocks*, p. 182. Hemphill, Austin, TX.

Furnes, H., Banerjee, N.R., Muehlenbachs, K., Staudigel, H. & de Wit, M. (2004). Early life recorded in Archaean pillow lavas. *Science* **304**, 578–581.

Furnes, H., Banerjee, N.R., Staudigel, H., Muehlenbachs, K., Simonetti, A., de Wit, M. & Van Kranendonk, M.J. (2006). Earth's oldest microbial biomarkers in pillow lavas: a new geological setting in the search for early life. *Geophys. Res. Abs.* **8**, 11078.

Gazzi, P. (1966). Le arenarie del flysch sopracretaceo dell'Appennino modenese; correlazioni con il flysch di Monghidoro. *Mineralogica Petrographica Acta* **12**, 69–97.

Hickman, A.H. (1975). Precambrian structural geology of part of the Pilbara region. *West. Aust. Geol. Survey Annual Report* 1974, pp. 68–73.

Hickman, A.H. (1983). Geology of the Pilbara block and its environs. *West. Aust. Geol. Survey Bull.* **127**, 268.

Hickman, A.H. (1984). Archean diapirism in the Pilbara Block, Western Australia. In *Precambrian Tectonics*, ed. Kroner, A. & Greiling, R.), pp. 113–127. E. Schweizerbarts'che Verlagsbuchhandlung, Stuttgart.

Hofmann, H.J. (2000). Archean stromatolites as microbial archives. In *Microbial Sediments* ed. Riding, R.E. & Awramik, S.M., pp. 315–327. Springer, Berlin.

Hoffman, H.J., Grey, K., Hickman, A.H. & Thorpe, R. (1999). Origin of 3.45 Ga coniform stromatolites in Warawoona Group, Western Australia. *Geol. Soc. Amer. Bull.* **111**, 1256–1262.

Ingersoll, R.V., Bullard, T.F., Ford, R.L., Grimm, J.P., Pickle, J.D. & Sares, S.W. (1984). The effect of grain size on detrital modes: a test of the Gazzi–Dickinson point-counting method. *J. Sed. Petrol.* **54**, 103–116.

Knoll, A.H. & Barghoorn, E.S. (1974). Ambient pyrite in Precambrian Chert: new evidence and a theory. *Proc. Natl Acad. Sci. USA* **71**, 2329–2331.

Lowe, D.R. (1980). Stromatolites 3,400-Myr old from the Archean of Western Australia. *Nature* **284**, 441–443.

Lowe, D.R. (1983). Restricted shallow-water sedimentation of early Archaean stromatolitic and evaporitic strata of the Strelley Pool Chert, Pilbara block, Western Australia. *Precamb. Res.* **19**, 239–283.

Lowe, D.R. (1994). Abiological origin of described stromatolites older than 3.2 Ga. *Geology* **22**, 387–390.

Nijman, W., De Bruin, K. & Valkering, M. (1998). Growth fault control of early Archaean cherts, barite mounds, and chert–barite veins, North Pole Dome, Eastern Pilbara, Western Australia. *Precamb. Res.* **88**, 25–52.

Schopf, J.W. (1992). The oldest fossils and what they mean. In *Major Events in the History of Life*, ed. Schopf, J.W., pp. 29–63. John and Bartlett, Boston.

Schopf, J.W. (1993). Microfossils of the Early Archaean Apex Chert: new evidence for the antiquity of life. *Science* **260**, 640–646.

Schopf, J.W. (1999). *The Cradle of Life*, p. 367. Princeton University Press, New York.

Schopf, J.W. & Packer, B.M. (1987). Early Archaean (3.3 billion to 3.5 billion-year-old) microfossils from Warawoona Group, Australia. *Science* **237**, 70–73.

Smithies, R.H., Van Kranendonk, M.J. & Champion, D.C. (2005). It started with a plume – early Archaean basaltic proto-continental crust. *Earth Planet. Sci. Lett.* **238**, 284–297.

Tice, M.M. & Lowe, D.R. (2004). Photosynthetic microbial mats in the 3,416-Myr-old ocean. *Nature* **431**, 549–552.

Van Kranendonk, M.J. (1999). North Shaw: Western Australia Sheet 2755. *West. Aust. Geol. Survey, 1:100 000 Geological Series*. Western Australia Geological Survey.

Van Kranendonk, M.J. (2000). Geology of the North Shaw 1:100,000 sheet. *West. Aust. Geol. Survey, 1:100 000 Geological Series Explanatory Notes*, p. 86. Western Australia Geological Survey.

Van Kranendonk, M.J. (2006). Volcanic degassing, hydrothermal circulation and the flourishing of early life on Earth: a review of the evidence from c. 3490–3240 Ma rocks of the Pilbara Supergroup, Pilbara Craton, Western Australia. *Earth Sci. Rev.* **74**, 197–240.

Van Kranendonk, M.J., Hickman, A.H., Smithies, R.H. & Nelson, D. (2002). Geology and tectonic evolution of the Archean North Pilbara Terrain, Pilbara Craton, Western Australia. *Econ. Geol.* **97**, 695–732.

Van Kranendonk, M.J., Hickman, A.H., Williams, I.R. & Nijman, W. (2001). Archean geology of the East Pilbara granite–greenstone terrain, Western Australia – a field guide. *West. Aust. Geol. Survey Record* **9**, 134.

Wacey, D., Kilburn, M., McLoughlin, N. & Brasier, M.D. (2006). The use of NanoSIMS to critically test claims of early (3.5 billion year old) life. *Geophys. Res. Abs.* **8**, 04906.

Walsh, M.M. (2004). Evaluation of early Archean volcaniclastic and volcanic flow rocks as possible sites for carbonaceous fossil microbes. *Astrobiology* **4**, 429–437.